ESD-TR-82-046

(12)

Technical Report 611

C.B. Chang
K.P. Dunn

A Functional Model for the Closely Spaced Object Resolution Process

20 May 1982

Prepared for the Department of the Army
under Electronic Systems Division Contract F19628-80-C-0002 by

Lincoln Laboratory
MASSACHUSETTS INSTITUTE OF TECHNOLOGY
LEXINGTON, MASSACHUSETTS

Approved for public release; distribution unlimited.

The work reported in this document was performed at Lincoln Laboratory, a center for research operated by Massachusetts Institute of Technology. This program is sponsored by the Ballistic Missile Defense Program Office, Department of the Army; it is supported by the Ballistic Missile Defense Advanced Technology Center under Air Force Contract F19628-80-C-0002.

This technical report has been reviewed and is approved for publication.

FOR THE COMMANDER

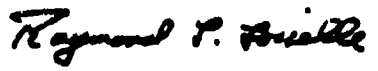

Raymond L. Loiselle, Lt.Col., USAF
Chief, ESD Lincoln Laboratory Project Office

MASSACHUSETTS INSTITUTE OF TECHNOLOGY
LINCOLN LABORATORY

A FUNCTIONAL MODEL FOR THE CLOSELY SPACED OBJECT RESOLUTION PROCESS

C.B. CHANG
K.P. DUNN
Group 32

TECHNICAL REPORT 611

20 MAY 1982

LEXINGTON MASSACHUSETTS

ABSTRACT

In this report, we describe a statistical model for characterizing the closely spaced object (CSO) resolution process. A logic for CSO clustering which simulates the CSO detection process is given. Measurement standard deviations for isolated targets, resolved CSO's, and unresolved CSO's are given. Results of this report are useful for functional simulation and performance analysis for the CSO resolution problem.

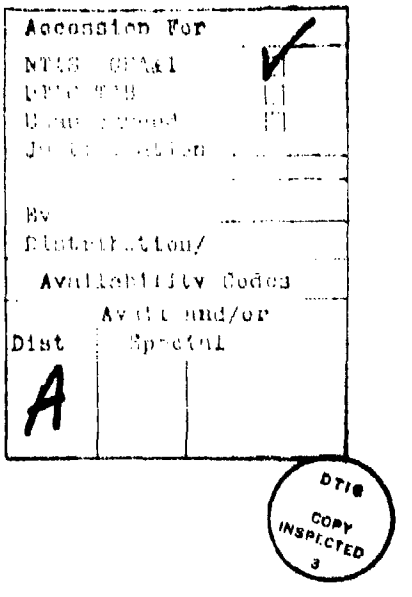

CONTENTS

I. INTRODUCTION

Resolution of closely spaced objects (CSO's) has been a subject of interest for many years first in radar applications and more recently with optical sensor applications. In our recent involvement in the optical signal processing area, it has often been necessary to obtain simulated signal processor outputs from an optical sensor. Because a complete focal plane/signal process (FP/SP) simulation is extremely complicated and time-consuming to carry out, a statistical functional model which simulates the above process is desirable.

In addition to the target signature which is a function of target orientation, sensor viewing angle, FP geometry, etc., the FP/SP process depends on many random factors such as background noise, target scintillation, sensor pointing error (determined by IMU and perhaps also stellar update, if available), receiver noise, etc. Functional models for most of these factors are available.* The only function which has not been modeled pertains to the process of resolution of closely spaced objects (CSO's), although the CSO problem itself and the performance of CSO resolution algorithms have been studied in considerable detail, [1]-[10]. The purpose of this report is to present a functional model for the CSO resolution process.

*For example, the SATIN program of Teledyne Brown Engineering, Huntsville, AL, and the FASSIM of MDAC, Huntington Beach, CA.

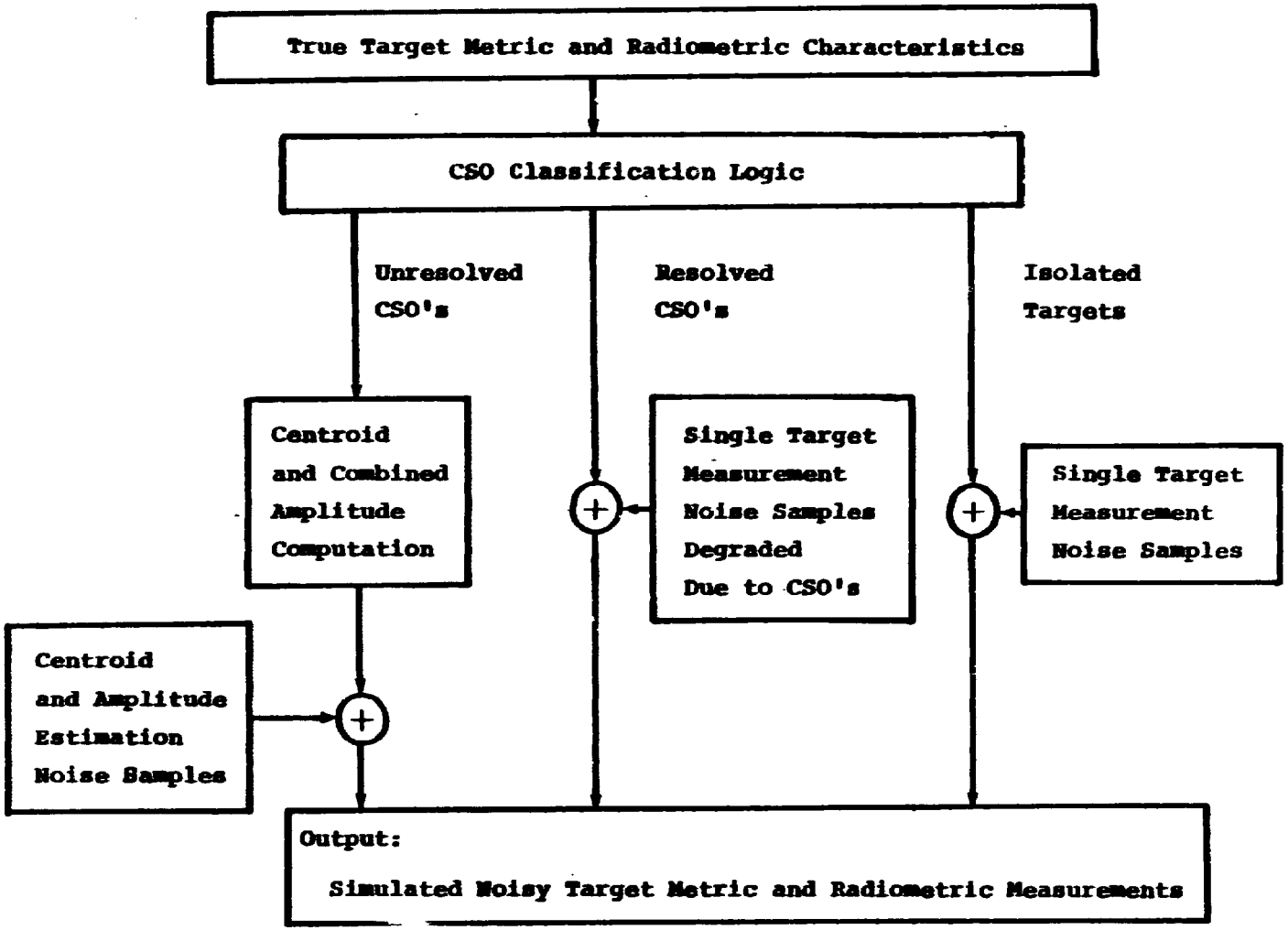

Fig. 1.1 CSO Functional Model Flow Diagram

A CSO functional model should consist of elements illustrated in Fig. 1.1. Notice that the CSO classification logic simulates the CSO detection process while the rest of the model simulates the metric and radiometric estimation errors in a CSO environment. These two procedures will be discussed in Section 2 and 3, respectively.

We emphasize that a functional model is a statistical simulator of the actual process. Such a model can never be made flawless because many processes can not be characterized with a parameterical statistical model. In some limited simulation studies (especially the metric measurement accuracy portion), we have obtained reasonable agreement with the functional model. We therefore believe that this model provides a good starting point for use as a signal processor simulator or to give analytical expressions for performance evaluation purposes.

Because our current involvement in the signal processing area has concentrated on the optical case, discussions in this report are centered around the resolution process for optical signals. It can be easily shown however, that this model can be extended to the radar case (in both range and angle domains) in a straightforward manner.

II. CSO CLASSIFICATION LOGIC

2.1 CSO Resolution Probability

The probability of correctly identifying the number of targets in a CSO cluster has been reported in several simulation studies, e.g., [3]. Roughly speaking, if the separation between targets is less than half of the detector width, the probability of identifying the existence of multiple targets is very small. If the separation is more than one detector width and the signal to noise ratio is 10 or higher, the probability of identification is very high while noticeable metric measurement degradation persists until the separation is greater than two detector widths. When the separation is between half to one detector width, the probability of CSO recognition is a function of separation and individual signal-to-noise ratio. Since an analytical expression for this probability does not exist, a precise functional model will include a numerical table containing resolution probabilities for a wide range of parameter values. The probability of recognizing a two-target CSO obtained from Monte Carlo simulation for several CSO configurations was shown in [3]. When the signal-to-noise ratio is high however, a straight lire between zero probability at half a detector width separation and unity probability at one detector width separation appears to be a good approximation for the resolution probability.

In summary, let P_{ij} denote the probability of resolving target i from target j; one may use

$$P_{ij} = \begin{cases} 1 & d_{ij} \geq 1 \text{ DW} \\ f(d_{ij}, SNR_i, SNR_j) & \frac{1}{2} \text{ DW} \leq d_{ij} \leq \text{DW} \\ 0 & d_{ij} \leq \frac{1}{2} \text{ DW} \end{cases} \tag{2.1}$$

where DW = detector width

d_{ij} = angular separation between target i and target j

SNR_k = voltage signal to noise ratio of the k^{th} target ($\geq$10).

For high SNR, one may approximate $f(\cdot,\cdot,\cdot)$ with

$$f(d_{ij}, SNR_i, SNR_j) = 1 - \frac{2d_{ij}}{DW} . \tag{2.2}$$

We note that when SNR is low, the probability of false CSO (i.e., deciding that two targets are present when in fact there is only one target) may become appreciable and should also be taken into account. The probability of false CSO can be reduced however, at the expense of probability of CSO detection (see the results of Ref. [3]). The probability of CSO detection and the probability of false CSO as functions of the target separation in detector widths are dependent upon the thresholds. Beyond the one detector width separation point, one can reduce the false CSO rate without reducing the probability of CSO detection. A more elaborate CSO functional model should include curves like those of Ref. [3].

2.2 CSO Clustering Logic

Given the angular locations of a set of targets, their pair-wise resolution probability can be evaluated using the above model. When a target is found to be resolved, the metric and radiometric measurements on this target are the true target location and amplitude, respectively, plus noise simulated by random numbers with known variances. When a target is unresolved, the centroid of unresolved targets is computed and the measured centroid is the true centroid corrupted by noise. The reported radiometric measurement will be the total signal amplitude at the true centroid location corrupted by noise. In the following, we describe a method for determining clusters of unresolved objects.

1) Two targets are called <u>connected</u> if they are <u>unresolved</u>.

2) Two targets are <u>completed resolved</u> if their separation is greater than two detector widths. If a target is completely resolved from all its neighboring targets, it is called an <u>isolated</u> target.

3) For two targets with their separation between 1/2 and 2 detector widths, they are either resolved or unresolved. For separation between 1 and 2 detector widths, they are <u>resolved</u>, but their metric and radiometric measurements must be degraded from that of an isolated target. For deciding on two targets with separation between 1/2 and 1 detector widths (i.e., $0 < P_{ij} < 1$), draw a uniform random number between

0 and 1. If this number is less than $f(d_{ij})$, they are resolved, otherwise they are unresolved. Metric measurements for resolved targets obtained this way must be degraded.

4) A cluster of objects are completely unresolved, if all objects in the cluster are mutually connected.

5) Each completely unresolved cluster will result in a centroid representing the metric location of all targets in the cluster.

An example of the above method is illustrated in Fig. 2.1. Notice that one centroid will be reported for each of the unresolved CSO clusters in Fig. 2.1, i.e., clusters 234, 345, 56, 68, and abcd. Each will have a centroid computed using true target amplitudes and locations. The measured centroid is the true centroid corrupted with noise samples. The target radiometric measurement is the combined signal amplitude at the centroid location corrupted with noise samples. The centroid and radiometric measurement computation will be discussed in the next section.

Finally, we remark that computer implementation of the above procedure is an interesting and artful subject. In the Appendix A, we present an algorithm and the IFTRAN listing of this algorithm which implements the CSO clustering logic.

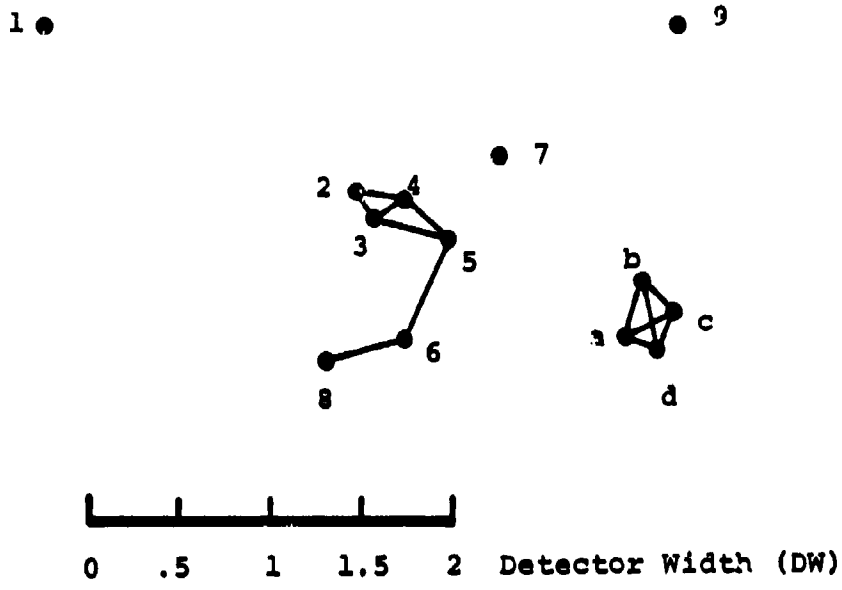

▲ Isolated Object: 1 (d > 2 DW's)

▲ Resolved CSO's: 7 (due to random draw)
9 (d > 1 DW)

▲ Unresolved CSO's:

△ Separations ≤ .5 DW:
234, 345, abcd

△ Separations between .5 and 1 DW, connected due to random draw:
56, 68

Fig. 2.1 CSO Classification Logic Illustration

III. CSO MEASUREMENT ACCURACY

3.1 Signal Model

Before we proceed to discuss the metric and radiometric measurement accuracy, we first establish notations and conventions useful for characterizing the signal process. We note that numerous studies have been devoted to understanding the optical signal process, see for example, [1] and [9]. These studies concluded that an additive Gaussian noise model is a good approximation for the background limited case. This is the model we will adopt in this report.

Let $s^+(t)$ denote the optical pulse shape appearing on the focal plane. The signal at the detector output is the convolution of $s^+(t)$ with the detector impulse response. We will use a rectangular pulse shape to denote the detector impulse response. The length of the rectangular pulse is called the "detector width". Let $s(t)$ denote the pulse shape at the detector output, for a symmetric pulse shape the matched filter impulse response is also $s(t)$. The matched filter output is therefore

$$\rho(t) = \int s(\tau)s(t-\tau)d\tau \qquad (3.1.1)$$

where $\rho(t)$ is also the signal autocorrelation function of $s(t)$ which is symmetric and contains unit energy, i.e.,

$$\int |s(t)|^2 dt = 1 \qquad (3.1.2)$$

Notice that we have used the notation "t" to denote the independent variable for the signal process. It denotes "time" in radar signals. For optical signals, it denotes "angle". We assume that the in-scan and cross-scan angle directions are orthogonal and can be treated independently.

We next define the root-mean-square (RMS) "bandwidth" (or beamwidth). The RMS bandwidth of a waveforem s(t) is the square root of the second central moment of P(iω), i.e.,

$$\begin{aligned} \beta &\triangleq \text{RMS "bandwidth"} \\ &= \int (\omega-\bar{\omega})^2 |P(i\omega)| d\omega \end{aligned} \qquad (3.1.3)$$

where $\bar{\omega}$ is the mean of $|P(i\omega)|$

$P(i\omega)$ is the Fourier transform of $\rho(t)$

$\rho(t)$ is the autocorrelation function of $s(t)$.

From (3.1.3) it can be shown that the square of the RMS bandwidth (or beamwidth) is equal to the negative of the second derivative of $\rho(t)$ evaluated at t=0, i.e.,

$$\beta^2 = - \ddot{\rho}(0) \qquad (3.1.4)$$

This relation will be used in later derivations.

It is often convenient to represent $\rho(t)$ using a Gaussian shaped function. In this case,

$$\rho(t) = e^{-t^2/2\sigma^2} \tag{3.1.5}$$

The Fourier transform of $\rho(t)$ is

$$P(i\omega) = \sqrt{2\pi}\,\sigma e^{-\sigma^2\omega^2/2} \tag{3.1.6}$$

the second central moment of $P(i\omega)$ is $1/\sigma^2$ and we can rewrite $\rho(t)$ as

$$\rho(t) = e^{-t^2\beta^2/2} \tag{3.1.7}$$

where β is the RMS bandwidth (beamwidth).

We now discuss the metric and radiometric measurement accuracy for isolated targets, resolved targets, and unresolved CSO's individually below.

3.2. Isolated Targets

An isolated target is a target free from interference induced by nearby targets. Its metric measurement accuracy is well-known and represented by

$$\sigma_o = \frac{\Delta\Theta}{SNR} \qquad (3.2.1)$$

where $\Delta\Theta$ is the sensor angular resolution and is equal to the inverse of the root-mean-square beamwidth of the detector output to a unit strength point source.

Similarly, the fractional signal amplitude (radiometric) measurement accuracy is inversely proportional to signal to noise ratio, i.e.,

$$\frac{\sigma_a}{a} = \frac{1}{SNR} \qquad (3.2.2)$$

where a is the signal amplitude.

3.3 Resolved CSO's

Metric measurement accuracy for resolved CSO's degrades from that for isolated targets. Assuming that the dominant degradation comes from the closest target, we will therefore only have to consider the two target case. Let $D(\tau)$ denote the degradation factor for a separation of τ; one obtains

$$\sigma_\theta = \sigma_o \cdot D(\tau) \qquad (3.3.1)$$

where σ_o is given in (3.2.1) and σ_θ is the degraded metric measurement accuracy. The degradation factor $D(\tau)$ is a function of the signal autocorrelation function. The exact expression for $D(\tau)$ is very complicated:

$$D(\tau) = \left[\frac{x_1 x_2 - x_3}{y}\right]^{1/2} \qquad (3.3.2)$$

where

$$x_1 = 1 - \rho(\tau)$$

$$x_2 = 1 + \rho(\tau)$$

$$x_3 = \dot{\rho}(\tau)^2/\beta^2$$

$$x_4 = 1 + \ddot{\rho}(\tau)/\beta^2$$

$$x_5 = 1 - \ddot{\rho}(\tau)/\beta^2$$

$$y = (x_1 x_5 - x_3)\ (x_2 x_4 - x_3)$$

$$\beta^2 = (\text{RMS bandwidth})^2 = -\ddot{\rho}(0).$$

The above expression can be obtained using the Cramer-Rao bound analysis illustrated in [1], [2], [7], [8] and [9]. If the signal autocorrelation function is Gaussian-shaped (eq. (3.1.7)), then the expression for $D(\tau)$ can be considerably simplified to obtain

$$D(\tau) = \left[\frac{1-(1+\tau^2\beta^2)\ \rho^2(\tau)}{(1-\rho^2(\tau))^2 - \tau^4\beta^4\rho^2(\tau)}\right]^{\frac{1}{2}} \qquad (3.3.3)$$

Similarly, the standard deviation of the degraded radiometric measurement, σ_r, can be expressed as

$$\sigma_r = \sigma_a \cdot D_a(\tau) \qquad (3.3.4)$$

A general expression for $D_a(\tau)$ is as follows:

$$D_a(\tau) = \left[\frac{(x_4 x_5 - x_3)}{y}\right]^{\frac{1}{2}} \qquad (3.3.5)$$

where x_3, x_4, and x_5 are the same as those defined for the degradation factor $D(\tau)$ in Eq. (3.3.2).

For a Gaussian-shaped $\rho(\tau)$, the $D_a(\tau)$ becomes

$$D_a(\tau) = \left[\frac{1-(1-\tau^2\beta^2 + \tau^4\beta^4)\rho^2(\tau)}{(1-\rho^2(\tau))^2 - \tau^4\beta^4\rho^2(\tau)}\right]^{\frac{1}{2}} \qquad (3.3.6)$$

where $\rho(\tau)$ is defined in (3.1.7).

The above gives the metric and radiometric measurement accuracy for the resolved CSO's. These formulas are obtained using the Cramer-Rao bound analysis. It has been observed that for targets separated by more than one half detector width, the performance of the maximum likelihood estimators is very close to that predicted with the Cramer-Rao bound, see for example [3] and [7]. Furthermore, the estimate is unbiased. We therefore believe that the above equations give a close indication of the actual performance.

3.4 Unresolved CSO's

For unresolved CSO's the centroid based upon the true signal amplitudes and locations and the combined signal amplitude at the centroid location will be computed. These quantities are then corrupted with noise samples to simulate metric and radiometric measurements for unresolved CSO's. This section gives formulas for computing the true and noisy centroids and signal

amplitudes. Notice now that the target metric and radiometric measurements have both bias and random errors.

Let (a_i,τ_i), i=1,...,N denote amplitudes and locations of unresolved CSO's arranged in either the in-scan or cross-scan direction. The matched filter output without noise is

$$r(t) = \sum_i a_i \rho(t-\tau_i) \qquad (3.4.1)$$

where $\rho(t)$ is the signal autocorrelation function. The centroid of $r(t)$, $\bar{t}$, is then

$$\bar{t} = \frac{\int t\, r(t)dt}{\int r(t)\,dt} \qquad (3.4.2)$$

Approximating $\rho(t)$ with a Gaussian pulse shape, one obtains the following expression for $\bar{t}$,

$$\bar{t} = \frac{\sum_i \tau_i a_i}{\sum_i a_i} \qquad (3.4.3)$$

We next consider the estimation accuracy. The received noisy measurement is

$$\tilde{r}(t) = r(t) + n(t) \qquad (3.4.4)$$

where $n(t)$ is Gaussian-white with variance N_o.

It is well-known that the Cramer-Rao bound on estimating $\bar{t}$ for problems defined by (3.4.4) is

$$\sigma_{\bar{t}} = \frac{1}{SNR \cdot \beta_r} \tag{3.4.5}$$

where

SNR = (voltage) signal-to-noise ratio

$$\triangleq ||r(t)||/\sqrt{N_o}$$

$||r(t)||$ = square root of signal energy

β_r = root-mean-square bandwidth of $r(t)$.

Let $\rho_r(\tau)$ denote the autocorrelation function of $r(t)$; then

$$\rho_r(\tau) = \frac{1}{||r(t)||^2} \int r(t)\, r(t+\tau)\, dt = \frac{1}{||r(t)||^2} \sum_i \sum_j a_i a_j \rho(\tau + \tau_{ij}) \tag{3.4.6}$$

where

$$\tau_{ij} = |\tau_i - \tau_j|$$

$\rho(\cdot)$ = autocorrelation function of $s(t)$

and

$$||r(t)||^2 = \sum_i \sum_j a_i a_j \rho(\tau_{ij}) \tag{3.4.7}$$

The root-mean-square bandwidth of $r(t)$, β_r is

$$\beta_r = (-\ddot{\rho}_r(0))^{1/2}$$

where $\ddot{\rho}_r(\tau)$ is the second derivative of the autocorrelation function $\rho_r(\tau)$, i.e.,

$$\ddot{\rho}_r(\tau) = \frac{1}{||r(t)||^2} \sum_i \sum_j a_i a_j \ddot{\rho}(\tau+\tau_{ij}) \qquad (3.4.9)$$

Substituting the above results into (3.4.5) one obtains

$$\sigma_{\bar{t}} = \frac{1}{\left[-\sum_i \sum_j SNR_i SNR_j \ddot{\rho}(\tau_{ij})\right]^{1/2}} \qquad (3.4.10)$$

where SNR_i is the signal-to-noise ratio of the i-th signal. For a Gaussian shaped $\rho(\tau)$, one has

$$\ddot{\rho}(\tau) = -\beta^2(1-\tau^2\beta^2)e^{-\tau^2\beta^2/2} \qquad (3.4.11)$$

where β is the root-mean-square bandwidth of $s(t)$. Finally, the centroid estimation accuracy is

$$\sigma_{\bar{t}} = \frac{1}{\left[\sum_i \sum_j SNR_i SNR_j \beta^2(1-\tau_{ij}^2\beta^2)e^{-\tau_{ij}^2\beta^2/2}\right]^{1/2}} \qquad (3.4.12)$$

With the above development, it is straightforward to obtain equations for radiometric measurements. The radiometric measurement for an unresolved CSO cluster is the combined signal amplitude at $\bar{\tau}$ corrupted with noise. The combined signal amplitude, denoted a_c, at $\bar{\tau}$ is

$$a_c = r(\bar{\tau}) \tag{3.4.13}$$

where $r(\cdot)$ is given in (3.4.1) and $\bar{\tau}$ is given in (3.4.2) (or (3.4.3)). The standard deviation on measuring a_c is

$$\frac{\sigma_{a_c}}{a_c} = \frac{1}{SNR} \tag{3.4.14}$$

where SNR is the same signal-to-noise ratio used in (3.4.5), i.e.,

$$SNR = ||r(t)||/\sqrt{N_o} \tag{3.4.15}$$

$$= \left[\sum_i \sum_j SNR_i SNR_j \rho(\tau_{ij})\right]^{1/2}$$

where SNR_i is the signal-to-noise ratio of the i-th signal and $\tau_{ij}=|\tau_i-\tau_j|$.

We note that when we use centroid location and amplitude to represent a group of targets, both location and amplitude estimates are biased with respect to each target, for example

$$b_{\tau_i} = \tau_i - \bar{t} \tag{3.4.16}$$

and

$$b_{a_i} = a_i - a_c \tag{3.4.17}$$

where b_{τ_i} and b_{a_i} are location and amplitude biases of the ith target, respectively. If one assumes a Gaussian shaped auto-correlation function, then for the two-target CSO case one obtains the location bias errors

$$b_{\tau_1} = \frac{-\ell}{R+1} \tag{3.4.18}$$

$$b_{\tau_2} = \frac{R\ell}{R+1} \tag{3.4.19}$$

and the amplitude bias errors

$$\frac{b_{a_1}}{a_1} = (1-e^{-\ell^2/2(R+1)^2}) - \frac{1}{R}\, e^{-R^2\ell^2/2(R+1)^2} \tag{3.4.20}$$

$$\frac{b_{a_2}}{a_2} = -R\, e^{-\ell^2/2(R+1)^2} + (1-e^{-R^2\ell^2/2(R+1)^2}) \tag{3.4.21}$$

where

$$R \triangleq a_1/a_2$$

$$\ell \triangleq \tau\beta \ .$$

The above equations can be easily extended to the multiple-target CSO case.

IV. NUMERICAL EXAMPLE

In this section, we will illustrate the CSO measurement accuracies for a two-target CSO case using the results of the previous section. We will assume that the single target matched filter output (or, the signal autocorrelation function) follows the Gaussian-shaped function. Furthermore, we use the conventional rule-of-thumb in which a signal to noise ratio of 10 results in an angle-splitting ratio of 10 (i.e., measurement accuracy is one tenth of the detector width), this results in detector width Δ DW = $1/\beta$.

We summarize pertinent measurement accuracy equations to be used in this section as a handy reference.

1. Target Location Estimation

1.1 Estimation Standard Deviation

1.1.1 Point Target:

$$\sigma_o = \frac{1}{\beta\ SNR} = \frac{\Delta\theta}{SNR}$$

1.1.2 Resolved CSO (Degradation Factor):

$$D(\ell) = \left[\frac{1-(1-\ell^2)\rho^2(\ell)}{1-\rho^2(\ell)-\ell^4\rho^2(\ell)}\right]^{1/2}$$

where

$$\ell = \tau\beta$$

τ = separation

$$\rho(\ell) = e^{-\ell^2/2}$$

1.1.3 Unresolved CSO (Centroid Degradation Factor For A Two-Target CSO)

$$D_u(\ell) = \frac{1}{[1+R^2+2R(1-\ell^2)e^{-\ell^2/2}]^{1/2}}$$

where

$$R = \frac{SNR_1}{SNR_2}$$

1.2 Estimation Bias (Two Target Case Normalized With Respect to $1/\beta$):

$$b_{\tau_1} = \frac{-\ell}{R+1}$$

$$b_{\tau_2} = \frac{R\ell}{R+1}$$

2. Target Amplitude Estimation

2.1 Estimation Standard Deviation

2.1.1 Point Target:

$$\frac{\sigma_a}{a} = \frac{1}{SNR}$$

2.1.2 Resolved CSO (Degradation Factor):

$$D_a(\ell) = \left[\frac{1-(1-\ell^2+\ell^4)\rho^2(\ell)}{(1-\rho^2(\ell))^2-\ell^4\rho^2(\ell)}\right]^{1/2}$$

2.1.3 Unresolved CSO (Centroid Degradation Factor For A Two-Target CSO):

$$D_{a_u}(\ell) = \left[\frac{1}{1+R^2+2Re^{-\ell^2/2}}\right]^{1/2}$$

2.2 Estimation Bias (Two Target Case):

$$\frac{b_{a_1}}{a_1} = (1-e^{-\ell^2/2(R+1)^2}) - \frac{1}{R}\, e^{-R^2\ell^2/2(R+1)^2}$$

$$\frac{b_{a_2}}{a_2} = -R\, e^{\ell^2/2(R+1)^2} + (1-e^{-R^2\ell^2/2(R+1)^2})$$

The metric and radiometric measurement accuracies for a two-target CSO case are illustrated in Figs. 4.1 and 4.2, respectively. In Fig. 4.1(a), we show the metric estimation random error degradation factor versus target separation in detector widths. When two targets are separated by more than one detector width, they are always resolved (provided that the SNR's are at least 10) and their location estimation error grows larger as the targets get closer. When two targets are closer than 1/2

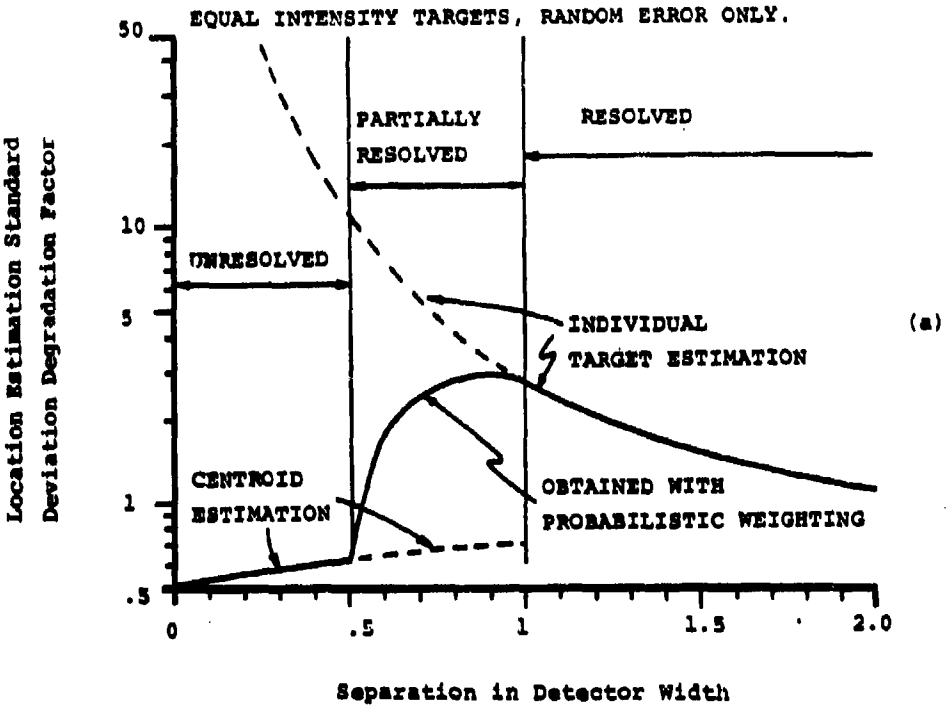

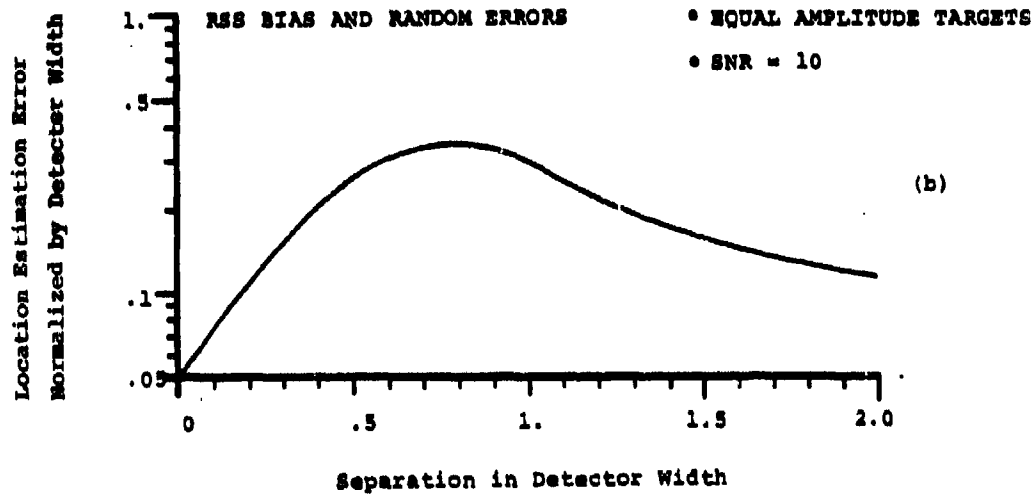

Fig. 4.1 CSO Metric (Target Location) Measurement Accuracy For a Two-Target Case

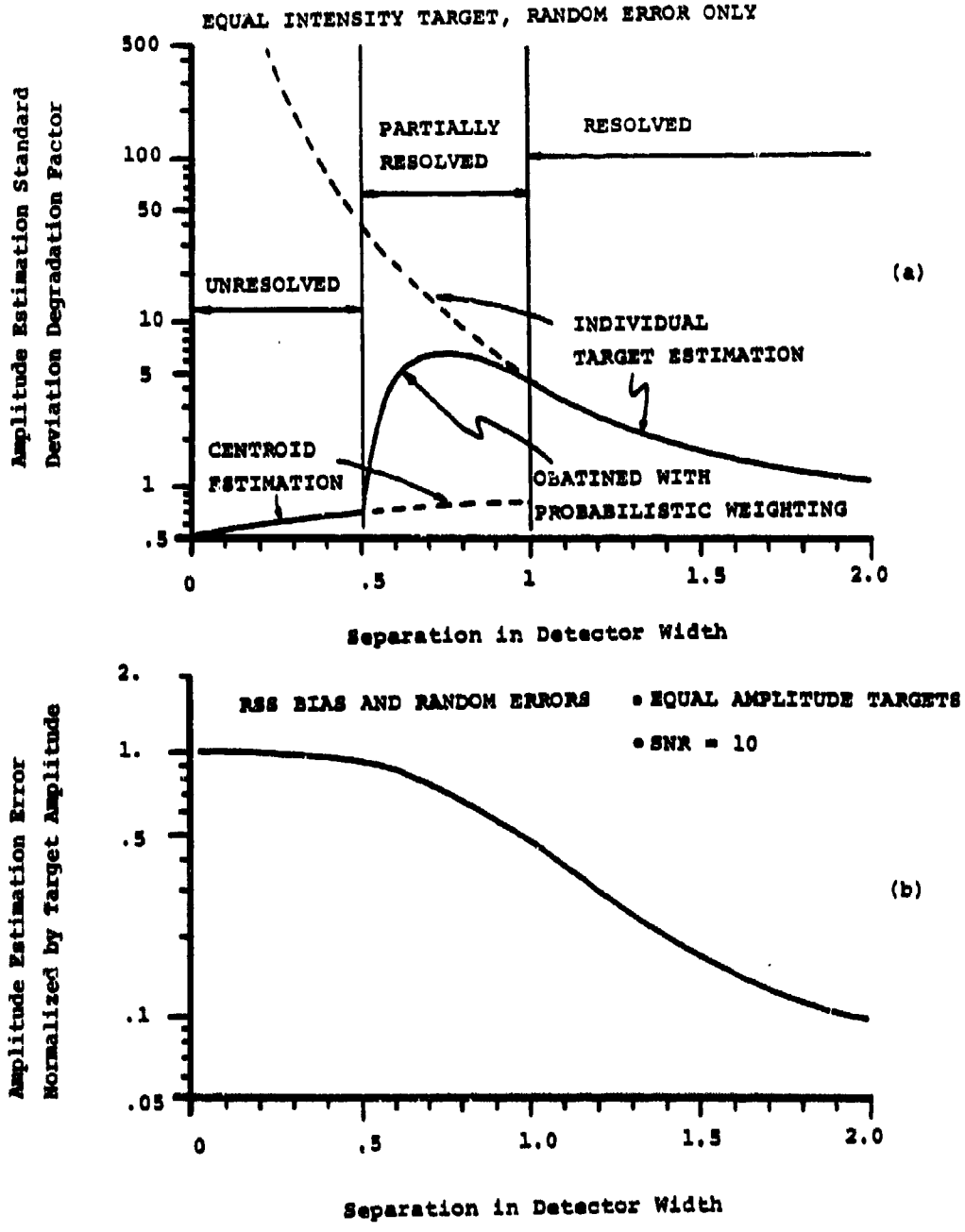

Fig. 4.2 CSO Radiometric (Target Intensity) Measurement Accuracy For a Two-Target Case

detector width, they are almost always unresolved and a single target is reported with its location being the centroid of these two targets. Because a combined two-target pulse will have a higher signal-to-noise ratio, the centroid estimation results in smaller random errors. When two targets are separated between one half and one detector width, they are sometimes resolved and sometimes unresolved. The curve in this region is obtained by combining the resolved and unresolved cases with probabilistic weightings. In Fig. 4.1(b), we compute the root-sum-square of the bias and the random errors. Recalling discussions of the previous section, the target location (and amplitude) estimate is unbiased when the targets are resolved. The bias term is therefore only included for targets separated by less than one detector width. Results of Fig. 4.1 seem to indicate that the position estimation accuracy improves when targets are closer than a certain distance. This is due to the fact that only one target is reported for a two-target CSO, in this situation the random error decreases as the combined signal to noise ratio increases and the bias error also decreases as target separation decreases. However, the estimate of the number of targets is in error which could degrade the scan-to scan correlation and tracking functions. This observation reinforces the fact that one must consider both detection and estimation processes in the CSO resolution problem. Figure 4.2 illustrates the amplitude estimation accuracy for a two-target CSO case. Most observations discussed for the position estimation

above still hold except that the bias error for the amplitude estimate increases as target separation decreases (compare 4.1(b) with 4.2(b)). When two equal intensity targets are almost co-located, the amplitude estimate bias error equals the target amplitude provided that the closer target does not block the farther target.

V. FINAL REMARKS

In this report, we have described a procedure for determining (1) CSO clusters and (2) metric and radiometric measurement accuracies for isolated, resolved, and unresolved targets. Target metric and radiometric measurements simulated this way (Fig. 1.1) include errors representative of the sensor and signal processor. The model discussed in this report is useful for functional simulation and error analysis. A numerical example illustrateing target parameter estimation accuracy for a two-target CSO case is given. These results also illustrate the transition between the completely resolved and unresolved regions for CSO targets.

APPENDIX A: AN ALGORITHM FOR IMPLEMENTING THE CSO CLUSTERING LOGIC*

In this appendix, we will give an algorithm for implementing the CSO clustering logic. Perhaps the best way of explaining this algorithm is to use examples. Consider the case that a group of 5 targets is being considered as potentially forming a CSO cluster. Let these five targets be referred to as target number 1 thru 5. After applying the target connection rules described in Section 2.2, we obtain the following CSO matrix:

$$\begin{pmatrix} 1 & 0 & 1 & 0 & 1 \\ 0 & 1 & 0 & 0 & 0 \\ 1 & 0 & 1 & 0 & 0 \\ 0 & 0 & 0 & 1 & 0 \\ 1 & 0 & 0 & 0 & 1 \end{pmatrix} \qquad \text{(A.1)}$$

The (i,j)th entry denotes the "status" between target i and target j. For example, the (1,3)th entry is "1"; this incidates that target 1 and target 3 are connected. A "0" entry denotes that two respective targets are resolved. Notice that all targets are connected to themselves (the diagonal terms). By visually examining this matrix, one can immediately conclude that targets 2 and 4 are completely resolved, targets 1 and 3 and targets 1 and 5 form two two-target CSO's. An algorithm for processing this matrix can proceed as follows:

*This implementation is due to L. Youens to whom we are very grateful.

1) At column one, search trhough the row elements; one first finds target 1 is connected with target 3.

2) Moving down again, one finds that target 5 is also connected with target 1. But target 5 is not connected with target 3, so targets 1, 3, and 5 do not form a complete connection.

3) Processing column two, one finds that target 2 is completely resolved.

4) Processing column three, one finds that targets 3 and 1 are connected. This result gives a redundant connection and this must be corss examined to avoid multiple measurements reported on the ame CSO cluster.

5) Processing column four, one finds that target 4 is completely resolved.

6) Processing column five, one finds that target 5 is connected with target 1.

The output of this algorithm will report four measurements, 13, 2, 4, and 15. In the above procedure, when one processes column i, one uses the (i,i)th element as the base element for comparison.

As a second example, we apply the above algorithm to process this following matrix

$$\begin{pmatrix} 1 & 0 & 1 & 0 & 1 \\ 0 & 1 & 0 & 0 & 0 \\ 1 & 0 & 1 & 0 & 1 \\ 0 & 0 & 0 & 1 & 0 \\ 1 & 0 & 1 & 0 & 1 \end{pmatrix} . \qquad (A.2)$$

One finds that targets 1, 3, and 5 form a complete connection. In this case, this algorithm reports 3 measurements consisting of 135, 2, and 4.

The following IFTRAN listing will process the i-th column of a CSO matrix:

```
C
C     KP, TARGET CSO MATRIX  (N,N)
C     NX, # OF TARGETS IN A CSO CLUSTER
C     IX(1) TO IX(NX), TARGET INDICES INTO KP ARRAY
C
      DO (I = 1, N)
         NX = 1
         IX(1) = I
         DO (K = 1, N)
C
C     KEY, SET TO 1 IF MATRIX ELEMENT ZERO OR IF TARGET
C          ALREADY IN IX ARRAY
C
```

```
                KEY = 0
                DO (L = 1, NX)
                    IF ( KP(IX(L),K) .EQ. 0
     &                  .OR. IX(L) .EQ. K ) KEY = 1
                END DO
                IF ( KEY .EQ. 0 )
                    NX = NX + 1
                    IX(NX) = K
                END IF
            END DO
C
C     OUTPUT CSO CLUSTER
C
            .
            .
            .
            .
        END DO
```

Notice that the I is the column index and K is the row index. Other key parameters are defined in the comment statements. Using this code to process the (A.2) matrix, one obtains the following results:

```
I=1,    NX=3,    IX(1)=1
                 IX(2)=3
                 IX(3)=5

I=2,    NX=1,    IX(1)=2

I=3,    NX=3,    IX(1)=3
                 IX(2)=1
                 IX(3)=5
```

```
I=4,    NX=1,    IX(1)=4

I=5,    NX=3,    IX(1)=5
                 IX(2)=1
                 IX(3)=3
```

Clearly, the 3-target CSO is reported three times. A simple cross check can quickly eliminate the redundant clusters.

ACKNOWLEDGMENTS

The authors are grateful to Dr. S. D. Weiner who has reviewed our manuscript several times and made suggestions which have guided the development of this work. We would also like to thank our colleague , L. Youens, whose talents, skills, and enduring interest have helped in putting many good ideas to work. The skillful typing and patience of Christine Tisdale were essential in preparation of the manuscript.

REFERENCES

[1] M. J. Tsai and K. P. Dunn, "Performance Limitations of Parameter Estimation of Closely Spaced Optical Targets Using Shot-Noise Detector Model," Technical Note 1979-35, Lincoln Laboratory, M.I.T. (13 June 1979), DDC AD-A073462.

[2] K. P. Dunn, "Accuracy of Parameter Estimates for Closely Spaced Optical Targets," Technical Note 1979-43, Lincoln Laboratory, M.I.T. (13 June 1979), DDC AD-A073093.

[3] M. J. Tsai, "Simulations Study on Detection and Estimation of Closely Spaced Optical Targets," Technical Note 1980-19, Lincoln Laboratory, M.I.T. (18 March 1980), DTIC AD-A088098/9.

[4] M. J. Tsai, "Sensitivity of Lens Aperatures on Estimation Accuracy of Optical CSO Parameters," private communication.

[5] M. J. Tsai, "Edge Effects for Optical Chevron Detectors", private communcation

[6] M. J. Tsai, "Resolution of Closely Spaced Optical Targets Using Maximum Likelihood Estimator and Maximum Entropy Method: A Comparison Study," TR-557, Lincoln Laboratory, M.I.T. (3 March 1981), DTIC AD-A100477

[7] R. W. Miller, "Accuracy of Parameter Estimates for Unresolved Objects," Technical Note 1978-20, Lincoln Laboratory, M.I.T. (8 June 1978), DDC AD-B028168.

[8] C. B. Chang, "Parameter Estimation Accuracy for Radar Targets Closely Spaced in Range," Technical Note 1980-46, Lincoln Laboratory, M.I.T. (12 November 1980), DDC AD-A094727/5.

[9] K. P. Dunn, "Accuracy of Parameter Estimates for Closely Spaced Optical Targets Using Multiple Detectors," Technical Report TR-589, Lincoln Laboratory, M.I.T. (23 October 1981), DTIC AD-A109185/9

[10] D. L. Fried, "Resolution, Signal-to-Noise Ratio and Measurements Precision, Optical Science Consultants, Report No. TR-034, October 1971, also published in J. Opt. Soc. Am., 69, 399 (1979).

REPORT DOCUMENTATION PAGE		READ INSTRUCTIONS BEFORE COMPLETING FORM
1. REPORT NUMBER ESD-TR-82-046	2. GOVT ACCESSION NO. AD-A116 410	3. RECIPIENT'S CATALOG NUMBER
4. TITLE (and Subtitle) A Functional Model for the Closely Spaced Object Resolution Process		5. TYPE OF REPORT & PERIOD COVERED Technical Report 6. PERFORMING ORG. REPORT NUMBER Technical Report 611
7. AUTHOR(s) Chaw-Bing Chang Keh-Ping Dunn		8. CONTRACT OR GRANT NUMBER(s) F19628-80-C-0002
9. PERFORMING ORGANIZATION NAME AND ADDRESS Lincoln Laboratory, M.I.T. P.O. Box 73 Lexington, MA 02173-0073		10. PROGRAM ELEMENT, PROJECT, TASK AREA & WORK UNIT NUMBERS Program Element Nos. 63304A and 63308A
11. CONTROLLING OFFICE NAME AND ADDRESS Ballistic Missile Defense Program Office Department of the Army 5001 Eisenhower Avenue Alexandria, VA 22333		12. REPORT DATE 20 May 1982 13. NUMBER OF PAGES 42
14. MONITORING AGENCY NAME & ADDRESS (if different from Controlling Office) Electronic Systems Division Hanscom AFB, MA 01731		15. SECURITY CLASS. (of this report) Unclassified 15a. DECLASSIFICATION DOWNGRADING SCHEDULE

16. DISTRIBUTION STATEMENT (of this Report)

Approved for public release; distribution unlimited.

17. DISTRIBUTION STATEMENT (of the abstract entered in Block 20, if different from Report)

18. SUPPLEMENTARY NOTES

None

19. KEY WORDS (Continue on reverse side if necessary and identify by block number)

closely spaced object (CSO) resolution process
statistical model
functional simulation
performance analysis

20. ABSTRACT (Continue on reverse side if necessary and identify by block number)

In this report, we describe a statistical model for characterizing the closely spaced object (CSO) resolution process. A logic for CSO clustering which simulates the CSO detection process is given. Measurement standard deviations for isolated targets, resolved CSO's and unresolved CSO's are given. Results of this report are useful for functional simulation and performance analysis for the CSO resolution problem.